

Nickel-Enhanced Solid-Phase Epitaxial Regrowth of Amorphous Silicon

B. Mohadjeri, J. Linnros,^(a) B. G. Svensson,^(b) and M. Östling

Royal Institute of Technology, Solid State Electronics, P.O. Box 1298, S-164 28 Kista-Stockholm, Sweden

(Received 2 October 1991; revised manuscript received 12 December 1991)

Low-temperature solid-phase epitaxial regrowth of amorphous silicon (*a*-Si) is reported for an ion-amorphized Ni/Si structure. The epitaxial regrowth follows after monosilicide formation upon heating to only 425 °C, as evidenced by Rutherford backscattering and channeling measurements and transmission electron microscopy. The regrowth rate of the *a*-Si layer (thickness ~600 Å) is enhanced by more than a factor of 300 compared with ordinary solid-phase epitaxy of ion-implanted *a*-Si. This is attributed to results from redistribution of Ni towards the *a*-Si/*c*-Si interface, as shown by secondary ion mass spectrometry, where the presence of Ni, or Ni-silicide nuclei, enhances the solid-phase epitaxy.

PACS numbers: 68.55.Ln, 61.70.At, 61.70.Bv, 61.80.Fc

As the dimensions of integrated circuit (IC) devices diminish metal silicides play an important role in the development of very-large-scale integrated (VLSI) technology. For example, silicides can be used as low resistivity contacts and for interconnect metallization. Among silicides that can be grown epitaxially on Si, cobalt disilicide has successfully been used as a dopant diffusion source in the manufacturing of ultrashallow (≤ 500 Å) n^+p and p^+n junctions [1], while nickel disilicide (NiSi₂) has the lowest lattice mismatch with Si, i.e., 0.4% [2]. On crystalline silicon (*c*-Si), NiSi₂ forms by a nucleation-controlled process at temperatures above 750 °C; once the silicide growth has been initiated silicide columns grow with extreme rapidity [3]. The resulting silicide layer exhibits, however, a rough surface and a corrugated silicide/silicon interface. This nonuniformity of the silicide layer and the high formation temperature severely limit the use of NiSi₂ in high-density IC fabrication where shallow dopant profiles are highly demanded.

Disilicides of both nickel and cobalt have, however, successfully been formed at low temperatures (~400 °C) on evaporated amorphous silicon (*a*-Si) films [4–6]. On *a*-Si, the NiSi₂ formation is diffusion controlled, and the additional free energy of *a*-Si compared to *c*-Si gives rise to a considerably larger negative formation energy of NiSi₂ on *a*-Si than on *c*-Si. This extra driving force may overcome the stress-strain and surface effects with the result of a lower formation temperature of NiSi₂.

Amorphous silicon may also be formed by a high-dose ion implantation [7]. However, on ion-amorphized Si layers, we have found that NiSi₂ does not form at low temperatures, and heat treatments over 750 °C are still required. We have investigated this difference in the formation of NiSi₂ on evaporated versus ion-implanted *a*-Si and, surprisingly, found that the ion-amorphized layer recrystallizes at temperatures (≤ 425 °C, for 1 h) much lower than those required for ordinary solid-phase epitaxy (SPE) (≥ 550 °C) of *a*-Si [8]. Low-temperature crystallization of *a*-Si has been reported previously for a few systems, mostly resulting in polycrystalline Si (poly-Si) formation. For example, high concentrations of indium resulted in a melt mediated growth of poly-Si [9]. Simi-

larly, aluminum and a few other metals have been shown to induce poly-Si nucleation at significantly reduced temperatures [10,11]. Furthermore, in recent studies Cammarata *et al.* [12] and Hayzelden, Batstone, and Cammarata [13] found that Ni-implanted *a*-Si films on thick thermally grown SiO₂ layers displayed an enhanced rate of single-crystal silicon formation, and it was suggested that the crystallization was catalyzed by migrating NiSi₂ precipitates. In the present case, however, the *a*-Si film crystallizes in an epitaxial process forming a continuous layer with the underlying *c*-Si as a seed. The low crystallization temperature is attributed to the presence of Ni, or Ni-silicide grains, in the *a*-Si layer at the *a*-Si/*c*-Si interface. This Letter reports on Ni-stimulated SPE by presenting Rutherford backscattering spectrometry (RBS), transmission electron microscopy (TEM), and secondary ion mass spectrometry (SIMS) measurements for heat-treated samples with Ni films on ion-amorphized Si.

3-in. *p*-type (100) silicon wafers of resistivity 3–45 Ω cm were cleaned in H₂SO₄, HNO₃, and HF solutions. Immediately after the cleaning procedure the wafers were inserted into an UHV system and nickel films were deposited using an electron gun evaporator. The base pressure was $\sim 10^{-8}$ Torr rising to $\sim 10^{-7}$ Torr during evaporation; the deposition rate was between 5 and 10 Å/s and the final film thickness was ~ 500 Å. The wafers were then implanted at room temperature using 380-keV ⁷⁵As⁺⁺ ions and a dose of 7×10^{14} ions/cm², resulting in an amorphous silicon layer extending ~ 1600 Å below the nickel film.

The resulting sample configuration, thus, consisted of 500-Å Ni on 1600-Å *a*-Si on a (100) Si substrate. Heat treatments were subsequently carried out in a vacuum furnace with a residual gas pressure in the low 10^{-7} range. The stoichiometry of the films was determined by RBS combined with the channeling using 2.4-MeV ⁴He⁺ ions. The TEM studies were performed in a JEOL JEM-2000 FX II instrument. The SIMS analyses were carried out in a Cameca IMS 4f microanalyzer, and the crater depths were measured using an Alphastep 200 stylus profilometer.

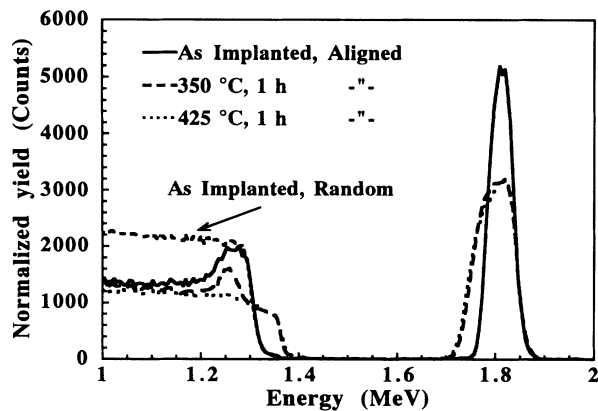


FIG. 1. Channeling spectra for the as-implanted sample and after heat treatments as 350 and 425 °C, for 1 h. The silicon signal height for the as-implanted sample taken in a random orientation is marked by the arrow. The four spectra have been normalized to the total counts in the Ni peak.

In Figs. 1 and 2 channeling spectra and TEM cross-sectional micrographs are shown, respectively, for an as-implanted sample and following heat treatments at 350 and 425 °C, for 1 h. The α -Si layer below the Ni film is clearly resolved in Figs. 1 and 2(a). The backscattering signal height for Si in this region coincides with the signal level recorded in a random orientation (indicated by the arrow in Fig. 1) revealing the amorphous nature of the buried α -Si layer.

After the heat treatment at 350 °C, ~ 1100 -Å NiSi has formed leaving ~ 600 -Å α -Si beneath the NiSi layer. As shown in Fig. 2(b) the NiSi layer exhibits a polycrystalline structure consisting of randomly oriented grains, resulting in a rough NiSi/ α -Si interface. The end of range damage caused by the implanted arsenic ions is identified as a dark band of defects lying just below the α -Si layer.

After annealing at 425 °C the top layer still consists of NiSi while there remains no α -Si below the NiSi layer, Figs. 1 and 2(c). As shown in the dark-field micrograph, taken from the same spot as in Fig. 2(c), the α -Si has completely regrown having the same orientation as the (100) Si substrate. Thus, the epitaxial regrowth takes place from the initial α -Si/ c -Si interface and occurs at a much reduced temperature compared with ordinary SPE. The SPE velocity obtained at 425 °C is ≥ 0.17 Å/s which is more than a factor of 300 larger than the ordinary SPE velocity at this temperature ($\sim 5 \times 10^{-4}$ Å/s) [8].

To certify that the observed low-temperature SPE was, in fact, caused by the presence of the top-layer Ni film a control experiment was performed on the as-implanted samples where the Ni film was etched off and heat treatments were subsequently carried out at 350 and 425 °C, for 1 h. Channeling spectra for the two heat treatments were almost identical and results before and after thermal annealing at 425 °C are shown in Fig. 3. A slight shar-

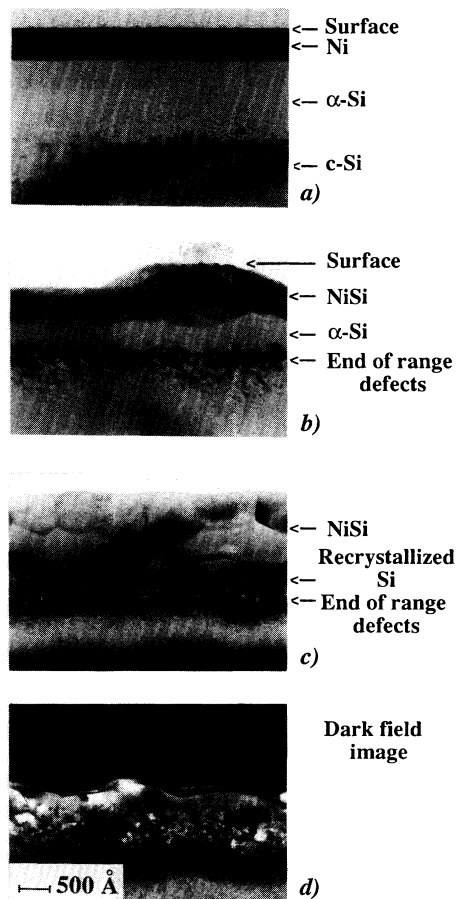


FIG. 2. TEM cross-sectional bright-field micrographs of (a) the as-implanted sample and after heat treatments at (b) 350 °C and (c) 425 °C. A dark-field image at (d) 425 °C is also included. For the 350 °C annealed sample, the overlaying glue and part of the silicide was, unfortunately, lost during sample preparation.

pening of the α -Si/ c -Si interface is observed after the heat treatment. The small Ni signal appearing in the spectra of Fig. 3 corresponds to $\sim 1 \times 10^{16}$ Ni atoms/cm² and is a result of some residual Ni oxide on the samples after the etching procedure.

To reveal whether Ni has diffused through the amorphous layer to the α -Si/ c -Si interface we performed SIMS measurements, and in Fig. 4 SIMS spectra are displayed for the samples heat treated at 350, 375, and 425 °C. The crater depth was carefully measured as a function of sputtering time for the sample structures used in Fig. 4, and a linear proportionality was found to hold with a correlation coefficient better than 0.998. Thus the depth scale in Fig. 4 was obtained by a linear conversion between sputtering time and crater depth, and despite the nonuniformity in the NiSi grain structure, as revealed by the TEM micrographs, the relative shift in the Ni tails shows a substantial diffusion of Ni (or Ni-silicide nuclei) in the α -Si layer at 375 °C. It is also interesting to note

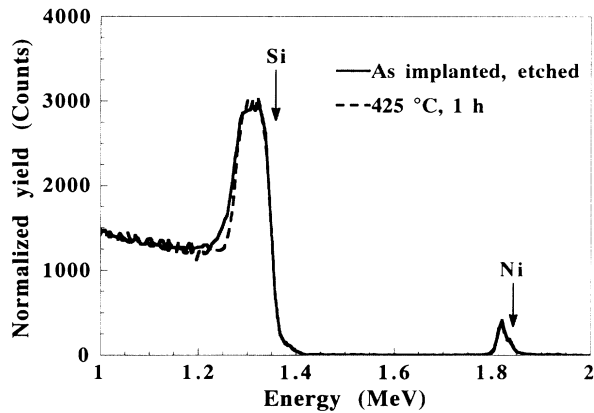


FIG. 3. Channeling spectra for an as-implanted sample where the top-layer Ni film was etched away, and following a heat treatment at 425 °C.

that the tail is smaller at 425 than at 375 °C showing a redistribution of Ni towards the surface during the SPE process.

The high Ni concentration in the *a*-Si layer or in the recrystallized Si, as revealed by the SIMS spectra in Fig. 4, should be present in the form of silicide precipitates, at least in the recrystallized Si layer. According to TEM, however, there is no clear evidence of such precipitates which should be visible, as indeed observed by Hayzelden, Batstone, and Cammarata [13], since NiSi₂ and *c*-Si have different absorption coefficients. Thus, the observed high Ni concentration is attributed to inhomogeneous grain size and film thickness of the original NiSi layer [cf. Figs. 2(b) and 2(c)] which would be averaged over the SIMS detection area (~60 μm in diameter).

The experimental data in Figs. 1–3 provide conclusive evidence that the presence of the top-layer Ni film results in a low-temperature regrowth of the underlying amorphized Si layer, and the following three models are possible candidates to explain this observation.

(1) A pure solid-phase epitaxial regrowth process enhanced by a high Ni concentration at the *a*-Si/*c*-Si interface. This requires significant diffusion of Ni through the amorphous Si before the SPE process is initiated. An enhanced SPE rate has been observed for layers containing dopants [8] and impurities such as gold [11]. In those experiments, however, the crystallization temperature was not significantly lowered as in the present case.

(2) Lateral SPE from silicide regions extending through the *a*-Si layer to the underlying bulk *c*-Si. This is supported in part by the TEM studies where, at a few locations [not shown in Fig. 2(b)], silicide grains extended down to the underlying *c*-Si. Furthermore, weak grain boundaries could be observed in the recrystallized layers [in micrographs similar to the one in Fig. 2(c)]. For this model to be valid, however, one must assume that the lateral SPE process is enhanced by a high Ni concentration, as in model (1), or by a process similar to the one in mod-

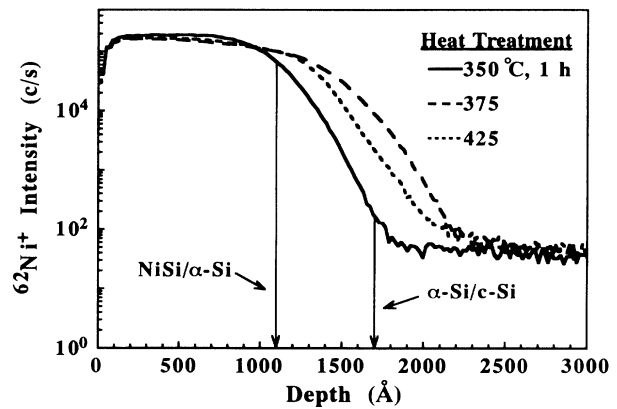


FIG. 4. SIMS depth profiles for heat treatments at 350, 375, and 425 °C, for 1 h. The ⁶²Ni⁺ secondary ion signal was recorded and the spectra were normalized to the integral ⁶²Ni⁺ intensity. The position of the NiSi/*a*-Si and *a*-Si/*c*-Si interfaces, as determined from the TEM micrograph in Fig. 2(b), is indicated on the depth axis.

el (3) below.

(3) Diffusion of Ni through the *a*-Si layer to the *a*-Si/*c*-Si interface followed by NiSi₂ formation at the interface. The NiSi₂ grains then migrate towards the NiSi layer transforming the passed *a*-Si into *c*-Si. This model was suggested by Erokhin *et al.* [14] from TEM studies of small NiSi₂ grains migrating through a buried *a*-Si layer. The moving grains would dissolve *c*-Si from their back interfaces (with respect to the direction of movement). The model is also in accordance with the works of Cammarata *et al.* [12] and Hayzelden, Batstone, and Cammarata [13] where Ni-rich regions were seen at the leading edges of recrystallized poly-Si needles. One may, however, question the presence of NiSi₂ grains since, according to nucleation theory, once they are formed, the complete system would be transformed into NiSi₂ being the more energetically favorable phase [3]. From our TEM studies we have not been able to find any NiSi₂ grains.

The SIMS data support both (1) and (3), and in the present RBS data we do not have high enough depth resolution to distinguish between the different models. Experiments on thicker *a*-Si layers are in progress to elucidate the appropriate mechanism.

To summarize, we have shown that a thin *a*-Si layer regrows epitaxially at a significantly lower temperature (< 425 °C) than ordinary SPE by the presence of a top NiSi layer. This is attributed to diffusion of Ni, or Ni-silicide nuclei, through the *a*-Si layer to the *a*-Si/*c*-Si interface where the presence of Ni promotes rapid SPE.

Dr. S. Johansson is greatly acknowledged for the TEM analysis and M. Mörsky for the arsenic implantation. The discussions with Professor F. M. d'Heurle are highly appreciated. The project was financially supported by the Swedish National Board for Technical Development.

- ^(a)Permanent address: Swedish Institute of Microelectronics, P.O. Box 1084, S-164 21 Kista-Stockholm, Sweden.
- ^(b)Present address: Department of Electrical Engineering, Australian National University, GPO Box 4, Canberra, ACT 2601, Australia.
- [1] R. Liu, F. A. Baiocchi, L. A. Heimbrook, J. Kovalchick, D. L. Malm, D. S. Williams, and W. T. Lynch, *Electrochem. Soc.* **87-11**, 446 (1987).
- [2] H. Ishiwara, S. Saitoh, and K. Hikosaka, *Jpn. J. Appl. Phys.* **20**, 843 (1981).
- [3] F. M. d'Heurle, *J. Mater. Res.* **3**, 167 (1988).
- [4] L. R. Zheng, L. S. Hung, and J. W. Mayer, *Mater. Res. Soc. Symp. Proc.* **54**, 579 (1986).
- [5] C.-D. Lien, M.-A. Nicolet, and S. S. Lau, *Phys. Status Solidi (a)* **81**, 123 (1984).
- [6] C.-D. Lien, M.-A. Nicolet, and S. S. Lau, *Appl. Phys. A* **34**, 249 (1984).
- [7] J. S. Williams and J. M. Poate, *Ion Implantation and Beam Processing* (Academic, Australia, 1984).
- [8] G. L. Olson and J. A. Roth, *Materials Science Reports* (North-Holland, Amsterdam, 1988), Vol. 3, pp. 1-78.
- [9] E. Nygren, J. C. McCallum, R. Thornton, J. S. Williams, and G. L. Olson, *Mater. Res. Soc. Symp. Proc.* **100**, 405 (1988).
- [10] G. Radnoczi, A. Robertsson, H. T. G. Hentzell, S. F. Gong, and M.-A. Hasan, *J. Appl. Phys.* **69**, 6394 (1991).
- [11] D. C. Jacobson, J. M. Poate, and G. L. Olson, *Appl. Phys. Lett.* **48**, 118 (1986).
- [12] R. C. Cammarata, C. V. Thompson, C. Hayzelden, and K. N. Tu, *J. Mater. Res.* **5**, 2133 (1990).
- [13] C. Hayzelden, J. L. Batstone, and R. C. Cammarata, *Appl. Phys. Lett.* **60**, 225 (1992).
- [14] Y. N. Erokhin, R. Grötzschel, S. R. Oktyabrsky, S. Rooda, W. Sinke, and A. F. Vjatkin, in *Proceedings of the European Materials Research Society, Strasbourg, France, 27-31 May 1991* (to be published).

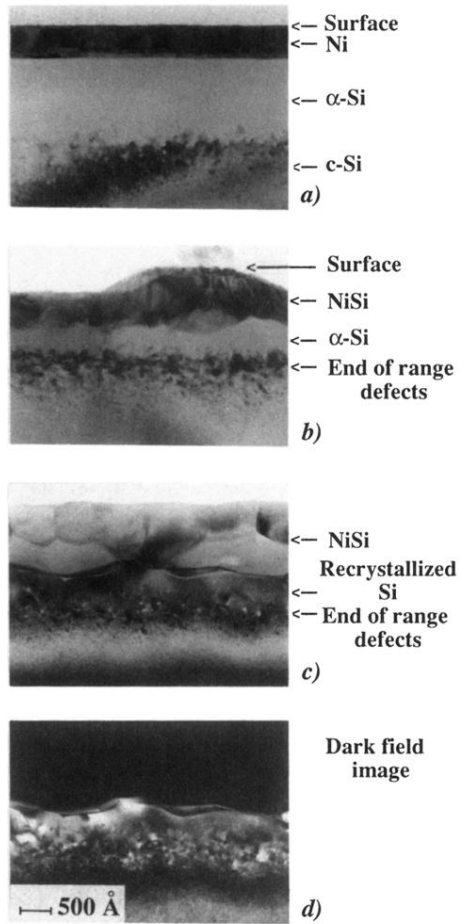


FIG. 2. TEM cross-sectional bright-field micrographs of (a) the as-implanted sample and after heat treatments at (b) 350°C and (c) 425°C. A dark-field image at (d) 425°C is also included. For the 350°C annealed sample, the overlaying glue and part of the silicide was, unfortunately, lost during sample preparation.